A ^{23}Na Magic Angle Spinning Nuclear Magnetic Resonance, XANES, and High-Temperature X-ray Diffraction Study of NaUO$_3$, Na$_4$UO$_5$, and Na$_2$U$_2$O$_7$

A. L. Smith,*,†,‡ P. E. Raison,*,† L. Martel,† T. Charpentier,§ I. Farnan,∥ D. Prieur,† C. Hennig,⊥ A. C. Scheinost,⊥ R. J. M. Konings,† and A. K. Cheetham‡

†European Commission, Joint Research Centre, Institute for Transuranium Elements, P.O. Box 2340, D-76125 Karlsruhe, Germany

‡Department of Materials Science and Metallurgy, University of Cambridge, 27 Charles Babbage Road, Cambridge CB3 0FS, United Kingdom

§CEA, IRAMIS, SIS2M, Laboratoire de Structure et Dynamique par Résonance Magnétique, UMR CEA/CNRS 3299, 91191 Gif-sur-Yvette, France

∥Department of Earth Sciences, University of Cambridge, Downing Street, Cambridge CB2 3EQ, United Kingdom, and

⊥Institute of Resource Ecology, Helmholtz Zentrum Dresden Rossendorf (HZDR), , P.O. Box 10119, 01314 Dresden, Germany

S *Supporting Information*

XANES spectra   *MAS-NMR*
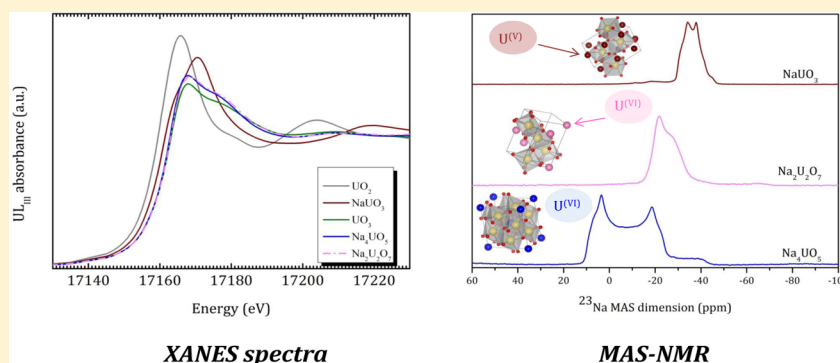
ABSTRACT: The valence state of uranium has been confirmed for the three sodium uranates NaU^{V}O$_3$/[Rn](5f^1), Na$_4$U^{VI}O$_5$/[Rn](5f^0), and Na$_2$U$^{VI}_2$O$_7$/[Rn](5f^0), using X-ray absorption near-edge structure (XANES) spectroscopy. Solid-state ^{23}Na magic angle spinning nuclear magnetic resonance (MAS NMR) measurements have been performed for the first time, yielding chemical shifts at −29.1 (NaUO$_3$), 15.1 (Na$_4$UO$_5$), and −14.1 and −19 ppm (Na1 8-fold coordinated and Na2 7-fold coordinated in Na$_2$U$_2$O$_7$), respectively. The [Rn]5f^1 electronic structure of uranium in NaUO$_3$ causes a paramagnetic shift in comparison to Na$_4$UO$_5$ and Na$_2$U$_2$O$_7$, where the electronic structure is [Rn]5f^0. A ^{23}Na multi quantum magic angle spinning (MQMAS) study on Na$_2$U$_2$O$_7$ has confirmed a monoclinic rather than rhombohedral structure with evidence for two distinct Na sites. DFT calculations of the NMR parameters on the nonmagnetic compounds Na$_4$UO$_5$ and Na$_2$U$_2$O$_7$ have permitted the differentiation between the two Na sites of the Na$_2$U$_2$O$_7$ structure. The linear thermal expansion coefficients of all three compounds have been determined using high-temperature X-ray diffraction: α_a = 22.7 × 10^{-6} K^{-1}, α_b = 12.9 × 10^{-6} K^{-1}, α_c = 16.2 × 10^{-6} K^{-1}, and α_{vol} = 52.8 × 10^{-6} K^{-1} for NaUO$_3$ in the range 298−1273 K; α_a = 37.1 × 10^{-6} K^{-1}, α_c = 6.2 × 10^{-6} K^{-1}, and α_{vol} = 81.8 × 10^{-6} K^{-1} for Na$_4$UO$_5$ in the range 298−1073 K; α_a = 6.7 × 10^{-6} K^{-1}, α_b = 14.4 × 10^{-6} K^{-1}, α_c = 26.8 × 10^{-6} K^{-1}, α_β = −7.8 × 10^{-6} K^{-1}, and α_{vol} = −217.6 × 10^{-6} K^{-1} for Na$_2$U$_2$O$_7$ in the range 298−573 K. The α to β phase transition reported for the last compound above about 600 K was not observed in the present studies, either by high-temperature X-ray diffraction or by differential scanning calorimetry.

■ INTRODUCTION

Sodium-cooled fast reactors (SFRs) have been selected as a promising concept for the next generation of nuclear reactors by the Generation IV International Forum (GIF).[1] From safety perspectives it is essential to gain a thorough knowledge of the potential products of reaction between the (U,Pu)O$_2$ mixed oxide fuel and the sodium coolant, as the two might come into contact in the event of a breach of the stainless steel cladding,

even though such events are extremely rare under normal operating conditions. Numerous studies have been carried out in the past to assess the direct consequences, including further cladding failure, restriction of the flow of coolant within a subassembly of fuel pins, or contamination of the primary

coolant with plutonium, minor actinides, or highly radioactive fission products.[2−4] As part of our program of research at the Joint Research Centre-Institute for Transuranium Elements (JRC-ITU, Karlsruhe, Germany), we are currently investigating the structural, thermomechanical and thermodynamic properties of the numerous compounds forming in the Na−U−O, Na−Np−O, and Na−Pu−O phase diagrams.[5−8]

We report herein a X-ray absorption near-edge structure (XANES), ^{23}Na magic angle spinning nuclear magnetic resonance (MAS NMR), and high-temperature X-ray diffraction study of $NaUO_3$, Na_4UO_5, and $Na_2U_2O_7$. XANES is a powerful technique to determine the valence state and coordination environment. ^{23}Na MAS NMR offers deep insight into the structure of the material, giving information on the number of Na sites, the structural order/disorder, the local Na coordination environment in terms of Na−O distances, and the degree of asymmetry of the coordination sphere.[9] Uranium has a $[Rn](5f^1)$ electronic configuration in $NaUO_3$ and a $[Rn](5f^0)$ electronic configuration in Na_4UO_5 and $Na_2U_2O_7$. The effect of unpaired f electrons on the ^{23}Na MAS NMR spectrum is particulary interesting and has been investigated here. We have also carried out density functional theory (DFT) calculations of NMR parameters using the DFT-GIPAW[10] (gauge including projector augmented wave) code, specifically devised to treat periodic solids: i.e., not limited to the cluster approach as recently described for UO_2^{2+}.[11] It is shown that for the diamagnetic phases Na_4UO_5 and $Na_2U_2O_7$ good agreement with the experimental data is obtained, offering interesting perspectives for future investigation of similar materials (though this approach is not yet applicable to paramagnetic phases). To the authors' knowledge, reports of the high-temperature behavior of these compounds are limited, if not nonexistent. The study of the materials' thermal expansion properties appears, however, to be a critical issue for the real-time modeling of the evolution of a pin failure in case of an accident.

■ RESULTS AND DISCUSSION

X-ray Diffraction and X-ray Absorption Near Edge Structure (XANES) Studies. All the details of the X-ray diffraction studies performed on the $NaUO_3$, Na_4UO_5, and $Na_2U_2O_7$ compounds are given in the Supporting Information. We have confirmed the known structures of $NaUO_3$[12] and Na_4UO_5.[13] $NaUO_3$ crystallizes in the orthorhombic system, space group $Pbnm$, with lattice parameters $a = 5.778(3)$ Å, $b = 5.909(3)$ Å, and $c = 8.284(3)$ Å, while Na_4UO_5 has a tetragonal structure, space group $I4/m$, with lattice parameters $a = 7.548(3)$ Å and $c = 4.637(3)$ Å. We have also found clear evidence that $Na_2U_2O_7$ is isostructural with $Na_2Np_2O_7$[6] and $K_2U_2O_7$,[14] i.e. monoclinic, in the space group $P2_1$ (with two Na sites which are 7- and 8-fold coordinated), and not rhombohedral $R\bar{3}m$ (with a 6-fold Na site) as reported in the literature.[15] The corresponding cell parameters were determined at $a = 6.887(3)$ Å, $b = 7.844(3)$ Å, $c = 6.380(3)$ Å, and $\beta = 111.29(5)°$. The unit cell volume is slightly greater for the uranium (321.2 Å^3) than for the neptunium compound (313.9 Å^3), which is consistent with the ionic radii of U^{6+} and Np^{6+}.[16]

XANES spectra of the three phases were collected at the U-L_{III} edge together with $U^{IV}O_2$[17] and $U^{VI}O_3$ reference compounds (Figure 1). The energy positions of the inflection points and of the white lines are provided in Table 1.

Soldatov et al.[18] already measured NaU^VO_3, and our results are in very good agreement with their work. The low-energy shoulder is an intrinsic feature of the uranium unoccupied (6d)
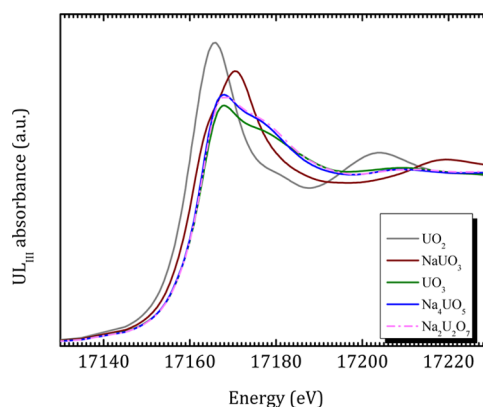
Figure 1. Normalized XANES spectra of $NaUO_3$, Na_4UO_5, and $Na_2U_2O_7$, together with those of the UO_2 and UO_3 reference compounds.

Table 1. Energies of the Inflection Points and White Lines of the U-L$_{III}$ XANES Spectra

sample	inflection point (eV)	white line (eV)
UO_2	17169.9(5)	17175.5(5)
$NaUO_3$	17170.4(5)	17180.1(5)
UO_3	17172.8(5)	17177.7(5)
Na_4UO_5	17172.7(5)	17177.6(5)
$Na_2U_2O_7$	17172.9(5)	17177.7(5)

electronic states of the U^V within the $NaUO_3$ phase.[18] The inflection points and white lines of Na_4UO_5 and $Na_2U_2O_7$ are perfectly aligned with those of $U^{VI}O_3$. A shoulder is also observed for these two compounds about 15 eV after the white line, a feature specific to U^{VI},[17] and no shoulder is found below it, as is the case for U^V.[18] Those results are consistent with uranium being exclusively in the oxidation state VI in Na_4UO_5 and $Na_2U_2O_7$ and therefore having a $[Rn]5f^0$ electronic shell.

^{23}Na Nuclear Magnetic Resonance Magic Angle Spinning (NMR-MAS) Measurements. ^{23}Na MAS NMR has proven to be an efficient tool to probe the local structure in a wide range of materials,[19,20] complementary to X-ray diffraction[21,22] for crystal structure investigation. The compounds $NaUO_3$ and Na_4UO_5 possess a single crystallographic site for Na. Their ^{23}Na MAS NMR spectra and fits are presented in Figure 2. The line shapes are typical of a powder second-order quadrupolar broadening, and the well-defined (i.e., sharp) singularities are indicative of well-ordered phases. For each compound, a single resonance is observed, in agreement with the X-ray diffraction data.[12,13]

The ^{23}Na signal of the 8-fold coordinated sodium in $NaUO_3$ was identified at −29.1 ppm, with a quadrupolar coupling constant C_Q and an asymmetry parameter η_Q equal to 1.7 MHz and 0.5, respectively (Table 2). This asymmetry parameter η_Q is consistent with the distorted NaO_8 octahedra. The isotropic chemical shift δ_{CS} of $NaUO_3$ was compared with those previously reported for other crystals (reference data of Mackenzie[20] and Ashbrook[23]) and is slightly outside the range expected for 8-fold coordination (Figure 7 in the Supporting Information). As the $NaUO_3$ compound is paramagnetic at room temperature ($\chi = 395 \times 10^{-6}$ emu mol^{-1}),[24] the variation of δ_{CS} at higher fields can be explained by a paramagnetic shift due to the pentavalent uranium ion ($5f^1$): i.e., following an interaction between sodium nuclei and unpaired electrons.[25,26]
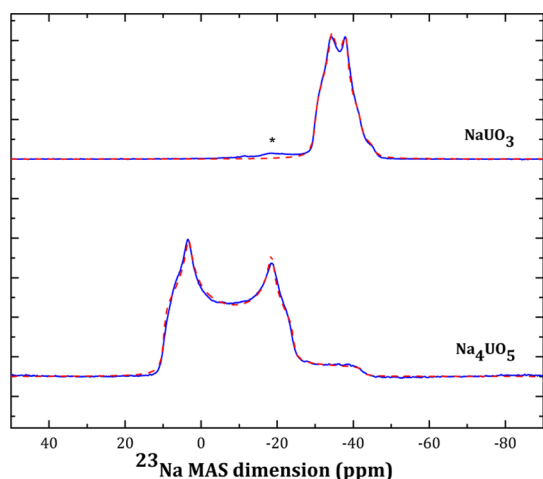
Figure 2. ^{23}Na MAS NMR spectra of NaUO$_3$ and Na$_4$UO$_5$ acquired at 15 kHz (blue line) and their corresponding fits (red dashed line). The asterisk corresponds to a sodium impurity also identified in the X-ray diffraction data.

Table 2. ^{23}Na Chemical Shifts (δ_{CS}), Quadrupolar Coupling Constants (C_Q), Asymmetry Parameters (η_Q), and the Quadrupolar Products (P_Q) of the Three Sodium Uranates

compd	δ_{CS} (ppm)	C_Q (MHz)	η_Q	P_Q (MHz)
NaUO$_3$	−29.1	1.7	0.5	1.9
Na$_4$UO$_5$	15.1	3.2	0.2	3.2
Na$_2$U$_2$O$_7$	−19			1.4
	−14.1			2.0

The ^{23}Na MAS NMR spectrum of the 6-fold coordinated sodium site in Na$_4$UO$_5$ was identified at 15.1 ppm and is in agreement with the fact that sodium atoms are surrounded by uranium(VI), where no paramagnetic shift contribution is

expected ($-20 \leq \delta_{CS}(\text{Na(VI)}) \leq +20$). A quadrupolar constant of 3.2 MHz and an asymmetry parameter of 0.2 were determined by fitting of the line shape. Such a low η_Q value is consistent with the symmetry of NaO$_6$, which is close to a regular octahedron (i.e., $\eta_Q = 0$ for cylindrical symmetry).

In contrast to the spectra of NaUO$_3$ and Na$_4$UO$_5$, the MAS NMR spectrum of Na$_2$U$_2$O$_7$ is featureless with a line shape (asymmetrical tail) suggesting structural disorder (Figure 3A). The synthesized compound was obtained with a rather poor crystallinity, as explained in the Supporting Information. Imperfect stoichiometry as a source of disorder was ruled out by the XANES results, which indicated pure U(VI) valence. A possible explanation could lie in the grain size of the synthesized product.

At first glance, the MAS NMR spectrum can be interpreted as a single site with local disorder. However, to gain more insight, a ^{23}Na multi quantum magic angle spinning (MQMAS) NMR study was performed (Figure 3B). MQMAS yields a two-dimensional spectrum in which the second-order quadrupolar anisotropic broadening is suppressed in the indirect dimension (isotropic dimension F$_1$), as is well illustrated by NaUO$_3$ (Figure 8 in the Supporting Information). The sheared 3QMAS spectrum of Na$_2$U$_2$O$_7$ is presented in Figure 3. The lower crystallinity of this compound is confirmed in the 2D spectrum by a distribution of chemical shift anisotropies. This spectrum can be compared with that of NaUO$_3$, which presents a well-defined quadrupolar line shape (Figure 8 in the Supporting Information). The direct differentiation between the two sodium sites of the monoclinic structural model is therefore not obvious at first sight. Nevertheless, the isotropic spectrum (free of anisotropic second-order quadrupolar broadening, as provided by a projection of the 2D MQMAS on the isotropic dimension) can be fitted using Gaussian line shapes identified at δ_{ISO} (corresponding to the isotropic shift in
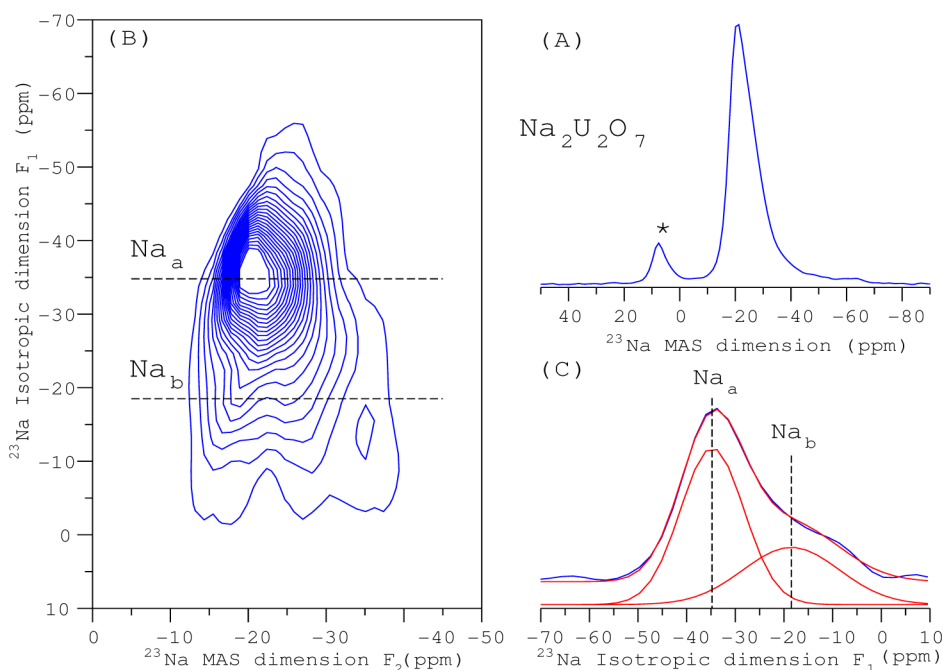
Figure 3. (A) ^{23}Na MAS NMR spectrum of Na$_2$U$_2$O$_7$ and (B) ^{23}Na MQMAS and (C) extracted isotropic dimension of the MQMAS for the Na$_2$U$_2$O$_7$ crystal acquired at 55 kHz on a 9.4 T NMR spectrometer. The asterisk corresponds to a sodium impurity also identified in the X-ray diffraction data.

the indirect dimension of the MQMAS) equal to −34.8 (Na$_a$) and −18.5 ppm (Na$_b$) (Figure 3C), respectively.

The occupancy of each site is found at 64% for Na$_a$ and 36% for Na$_b$. This deviation from 1:1 can be explained by the nonquantitativity of the MQMAS experiment.[27] Using slices extracted at these values of δ_{ISO}, the values of the total isotropic shift (i.e., the center of gravity) of the central transition (δ_{MAS}) can be determined for each site, yielding −23.5 (Na$_a$) and −23.4 ppm (Na$_b$), respectively. Given its complex shape, a precise fitting of the MQMAS spectrum is difficult and was not attempted. Nevertheless, the shift δ_{ISO} and δ_{MAS} can be used to obtain δ_{iso} and P_Q (the quadrupolar product) without fitting the MQMAS spectrum. For a spin $^3/_2$, one can obtain the two values using the equations[28,29]

$$\delta_{MAS} = \delta_{iso} - (\nu_Q^2 10^6)/(10\nu_0^2) \tag{1}$$

$$\delta_{ISO} = 17\delta_{iso}/8 + (\nu_Q^2 10^6)/(8\nu_0^2) \tag{2}$$

with $I = ^3/_2$. ν_Q is the quadrupolar frequency ($\nu_Q = 3C_Q(1 + 2\eta/3)^{1/2}/2I(2I - 1)$), and ν_0 is the Larmor frequency. Applying eq 1, δ_{iso} was found to be equal to −19 (Na$_a$) and −14.1 ppm (Na$_b$), and P_Q to be equal to 1.4 (Na$_a$) and 2.0 MHz (Na$_b$), respectively. The order of magnitude of P_Q values is consistent with that found for NaUO$_3$ and Na$_4$UO$_5$ (Table 2).

As the compounds Na$_4$UO$_5$ and Na$_2$U$_2$O$_7$ have no unpaired electrons (5f^0 shell, U^{VI}), they offer the opportunity to assess DFT calculations of NMR parameters.[9,30] As shown in Figures 4 and 5, a good correlation is obtained by plotting the
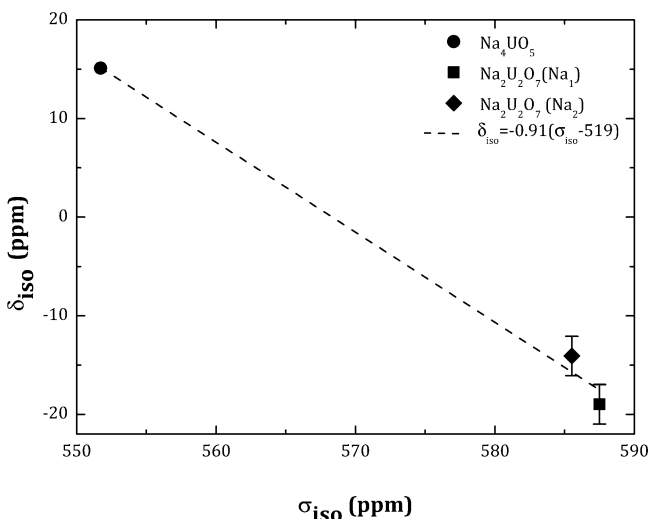
Figure 4. Experimental ^{23}Na isotropic chemical shift δ_{iso} versus theoretical isotropic shielding σ_{iso}. The dashed line is the linear fit.

experimental isotropic chemical shift against the theoretical isotropic chemical shielding (σ_{iso}), with a slope of 0.91. This shows that such calculations can predict well the observed difference in δ_{iso}. Linear regression analysis provides the reference isotropic chemical shielding (σ_{ref}) (the intercept value) yielding σ_{ref} = 519 ppm. On this basis, one can now attribute the two sodium sites in Na$_2$U$_2$O$_7$, where Na$_a$ corresponds to Na2 (NaO$_7$ 7-fold coordinated) and Na$_b$ to Na1 (NaO$_8$ 8-fold coordinated), using the same notation as for Na$_2$Np$_2$O$_7$ in the work of Smith et al.[6] (Table 3 in the Supporting Information). Hereafter, the two sodium sites in
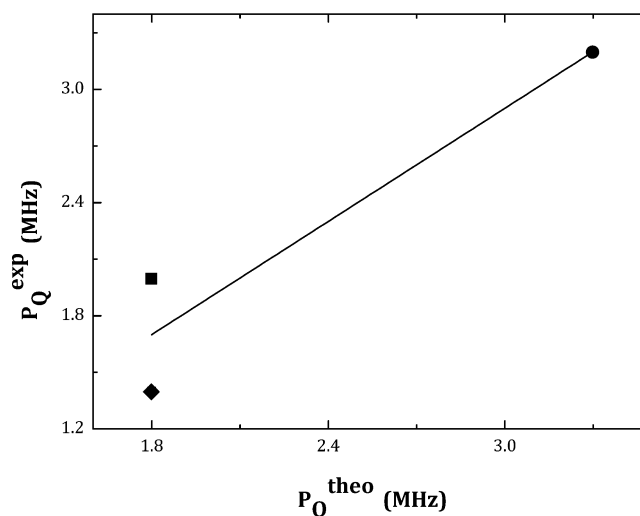

**Figure 5.** Experimental versus theoretical quadrupolar product P_Q. The solid line has a slope of unity.

Na$_2$U$_2$O$_7$ have been simply named Na1 and Na2 in the following discussion.

The quadrupolar parameters were also calculated, yielding 3.3, 1.8, and 1.8 for Na$_4$UO$_5$ and the two sodium sites in Na$_2$U$_2$O$_7$. The η_Q values corresponding to Na$_4$UO$_5$ and Na1 and Na2 in Na$_2$U$_2$O$_7$ are 0.14, 0.26, and 0.18, respectively. A good agreement was found for Na$_4$UO$_5$ with C_Q and η_Q close to the experimental values. Interestingly, for Na1 and Na2, the calculations could not differentiate between both C_Q parameters, and considering an uncertainty of ±0.1 (determined from Na$_4$UO$_5$) the η_Q values are in the same range. For Na$_2$U$_2$O$_7$, given the known high sensitivity of NMR to slight structural variations, this discrepancy can be ascribed to the structural models used in our calculation that would need further refinement, especially to account for the disorder as revealed by the MQMAS spectrum (Figure 3).

A linear decrease of δ_{iso} with increasing site size was observed in several sodium compounds.[9,21] Similarly, the isotropic chemical shift is plotted against the mean Na−O bond distance (denoted $\langle$Na−O$\rangle$) in Figure 6. A decrease of δ_{iso} with increasing $\langle$Na−O$\rangle$ is observed for the four Na sites. Nevertheless, due to its additional paramagnetic shift, the sodium site in NaUO$_3$ is not aligned with the three other Na sites of the nonmagnetic compounds. Considering only the latter, a regression line of $\delta_{iso} = -96(\langle$Na−O$\rangle) + 250$ (R = 0.999) is obtained. By placing its $\langle$Na−O$\rangle$ bond length on this line, one can obtain a rough estimate of the isotropic chemical shift (i.e., isotropic shift free of paramagnetic interaction) of NaUO$_3$. A δ_{iso} value of −7 ppm is obtained, suggesting a paramagnetic shift of −22 ppm.

High-Temperature Behavior. *NaUO$_3$.* To our knowledge, the only high-temperature X-ray diffraction experiment reported in the literature on NaUO$_3$ is one by Sali et al.[31] The aforementioned study goes up to 973 K, while the present study extends the range of temperatures up to 1373 K. Up to 1273 K, no change in crystal structure was observed except for a shift to lower 2θ following the expansion of the unit cell. At 1373 K, NaUO$_3$ started to decompose into Na$_2$U$_2$O$_7$ and UO$_2$. A possible reaction of decomposition is given by

$$3\text{NaUO}_3(s) \rightarrow \text{Na}_2\text{U}_2\text{O}_7(s) + \text{UO}_2(s) + \text{Na}(g) \tag{3}$$
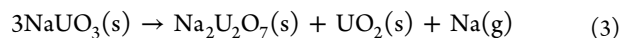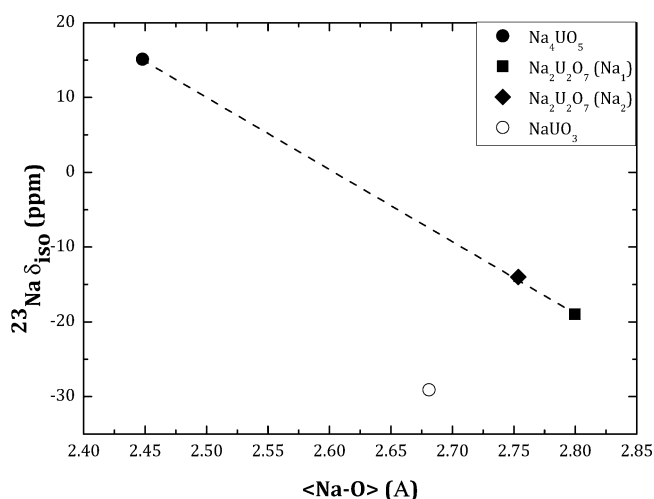
Figure 6. Evolution of the ^{23}Na isotropic chemical shift, δ_{iso}, as a function of the mean $\langle$Na$-$O$\rangle$ bond length. The dashed line represents the linear regression obtained for the nonmagnetic compounds and is given by $\delta_{iso} = -96(\langle$Na$-O\rangle) + 250$.

The evolution of the lattice parameters with temperature (Figure 7) was fitted by linear regression. The experiment
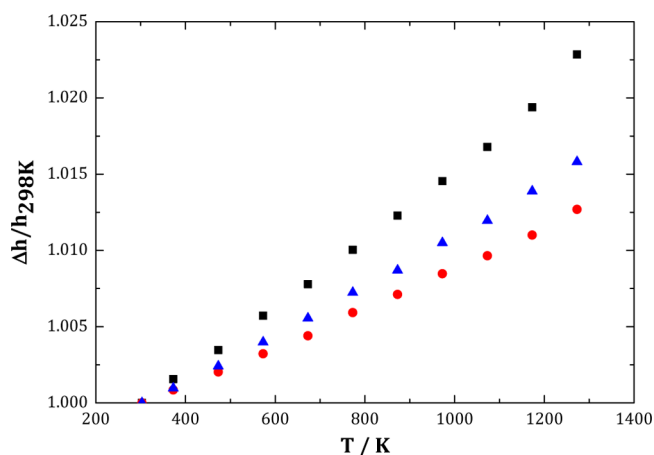
Figure 7. Evolution of the a (Å) (■), b (Å) (red ●) and c (Å) (blue ▲) cell parameters of NaUO$_3$ as a function of temperature.

showed that the cell parameters increased with temperature in all three directions. The corresponding linear thermal expansion coefficients were calculated using eq 4.

$$\alpha_a = \frac{1}{a_{298}}\frac{\partial a}{\partial T} \quad \alpha_b = \frac{1}{b_{298}}\frac{\partial b}{\partial T} \quad \alpha_c = \frac{1}{c_{298}}\frac{\partial c}{\partial T} \tag{4}$$

The values obtained were $\alpha_a = 22.7 \times 10^{-6}$ K^{-1}, $\alpha_b = 12.9 \times 10^{-6}$ K^{-1}, $\alpha_c = 16.2 \times 10^{-6}$ K^{-1}, and $\alpha_{vol} = 52.8 \times 10^{-6}$ K^{-1} for the temperature range 298$-$1273 K. Sali et al.[31] reported $\alpha_a = 22.74 \times 10^{-6}$ K^{-1}, $\alpha_b = 9.34 \times 10^{-6}$ K^{-1}, $\alpha_c = 15.69 \times 10^{-6}$ K^{-1}, and $\alpha_{vol} = 45.71 \times 10^{-6}$ K^{-1} in the temperature range 298$-$973 K.

Na$_4$UO$_5$. There is no report in the literature of high-temperature diffraction experiments carried out on Na$_4$UO$_5$. No change in crystal structure was observed up to 1073 K. NaUO$_3$ appeared at 1273 K and was obtained as the major

phase upon cooling. We suggest the possible decomposition reaction (5) to explain the occurrence of the latter compound.

$$Na_4UO_5(s) = NaUO_3(s) + 3Na(g) + O_2(g) \tag{5}$$
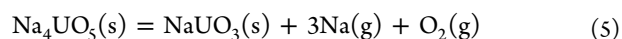
Using eqs 4, the linear thermal expansion coefficients were estimated along the crystallographic axes up to 1073 K (Figure 9 in the Supporting Information): $\alpha_a = 37.1 \times 10^{-6}$ K^{-1}, $\alpha_c = 6.2 \times 10^{-6}$ K^{-1}, and $\alpha_{vol} = 81.8 \times 10^{-6}$ K^{-1}. The expansion is significant along the a and b directions and limited along the c direction. This evolution can be explained in relation to the particular structure of Na$_4$UO$_5$. The UO$_6$ octahedra being oxygen bonded along the c axis, there is limited space for expansion in this direction, in contrast to the a and b directions. The expansion is related to the stretching of the Na$-$O distances. At 873 K the unit cell parameters obtained were $a = 7.703(3)$ Å and $c = 4.654(3)$ Å. Table 3 gives the atomic

Table 3. Refined Atomic Positions in Na$_4$UO$_5$ at 873 K^a

atom	oxidn state	Wyckoff	x	y	z	B_0 (Å^2)
Na	+1	8h	0.5931(5)	0.1999(5)	0	2.38(1)
U	+5	2a	0	0	0	0.57(1)
O1	−2	2b	0	0	0.5	1.39(1)
O2	−2	8h	0.2551(5)	0.0766(5)	0	3.72(1)

$^a R_{wp} = 9.50$.

positions at 873 K. Between room temperature and 873 K, it is mainly the distance U$-$O2 that increased, from 1.93(1) to 2.05(1) Å. Na$-$O2 remained constant at 2.36(1) Å, and Na$-$O1 increased from 2.38(1) to 2.42(1) Å. As a final point the distance U$-$O1 exhibited a minor change, from 2.32(1) to 2.33(1) Å due to expansion of the cell parameters. The positions of U and O1 are not refinable.

Na$_2$U$_2$O$_7$. Cordfunke et al.[32] performed thermodynamic measurements on Na$_2$U$_2$O$_7$ in 1982, comprising low-temperature (5 to 350 K) heat capacity determinations by adiabatic calorimetry and enthalpy increments in the range 390$-$926 K by drop calorimetry. The authors reported a slow (α to β) phase transition for the compound above about 600 K. In the present study, the Na$_2$U$_2$O$_7$ compound was carefully prepared as described in their publication, in particular with an annealing treatment in oxygen at 500 K, below the α to β phase transition. High-temperature X-ray diffraction measurements were subsequently carried out so as to visualize the transition and determine the coefficients of thermal expansion.

The X-ray diffraction pattern did not show any significant changes up to 773 K, except for a shift to lower 2θ caused by the thermal expansion of the unit cell. At 873 K, NaUO$_3$ appeared which formed according to the decomposition reaction (6). At 973 K, Na$_2$U$_2$O$_7$ had completely disappeared, and UO$_2$ was detected at 1073 K following the decomposition of NaUO$_3$.

$$Na_2U_2O_7(s) = 2NaUO_3(s) + {}^1/_2O_2(g) \tag{6}$$
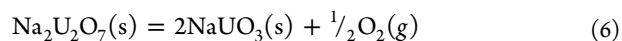
The materials' coefficients of thermal expansion were estimated up to 573 K, yielding $\alpha_a = 6.9 \times 10^{-6}$ K^{-1}, $\alpha_b = 17.3 \times 10^{-6}$ K^{-1}, $\alpha_c = 29.8 \times 10^{-6}$ K^{-1}, $\alpha_\beta = -9.5 \times 10^{-6}$ K^{-1}, and $\alpha_{vol} = -217.6 \times 10^{-6}$ K^{-1} (Figure 10 in the Supporting Information).

From the present experiment, we could not confirm the existence of an α to β phase transition above about 600 K. The latter transition could not be detected in our DSC experiments either, when the sample was heated to 923 K at various heating rates (5, 7, and 10 K/min). A possible explanation could lie in the very slow kinetics of the transition. In the drop calorimetry experiments performed by Cordfunke et al.,[32] the $Na_2U_2O_7$ sample was kept isothermal for several hours in a closed container before being "dropped" at 298 K. In this case, the prolonged heating at constant temperature could allow the formation of the α and β forms of the compound.

The coefficients of thermal expansion of all three phases are larger than for uranium oxide ($\alpha_{vol} = 32.4 \times 10^{-6}$ K^{-1} in the temperature range 298–1600 K[33]). This means that local swelling could be a real issue in case of a clad breach and sodium coolant–fuel interaction, potentially inducing further cladding failure.

CONCLUSIONS

The present work illustrates the powerful combination of MAS NMR and MQMAS in materials chemistry studies, as a complementary tool to X-ray diffraction and as a signature for paramagnetic phases with an unpaired number of 5f electrons.

The particular $[Rn](5f^1)$ electronic structure of uranium in $NaUO_3$ causes a paramagnetic shift in the ^{23}Na MAS NMR spectrum: the chemical shift was recorded at −29.1 ppm. The quadrupolar coupling constant C_Q was 1.7 MHz and the asymmetry parameter 0.5, consistent with the distortion of the NaO_8 octahedron. The coefficients of linear thermal expansion of $NaUO_3$ were estimated at $\alpha_a = 22.7 \times 10^{-6}$ K^{-1}, $\alpha_b = 12.9 \times 10^{-6}$ K^{-1}, $\alpha_c = 16.2 \times 10^{-6}$ K^{-1}, and $\alpha_{vol} = 52.8 \times 10^{-6}$ K^{-1} in the temperature range 298−1273 K.

XANES studies carried out for the first time on Na_4UO_5 and $Na_2U_2O_7$ have confirmed the hexavalent state of uranium in those compounds and therefore the $[Rn](5f^0)$ electronic configuration. The ^{23}Na MAS NMR spectrum of Na_4UO_5 yielded a chemical shift at 15.1 ppm consistent with the hexavalent uranium. C_Q was 3.2 MHz in this case and η_Q 0.2, as expected for the regular NaO_6 octahedron. The thermal expansion is high along the a and b directions ($\alpha_a = 37.1 \times 10^{-6}$ K^{-1}), and limited along the c direction ($\alpha_c = 6.2 \times 10^{-6}$ K^{-1}) as a consequence of the oxygen bonding of the UO_6 octahedra along c and of the (probable) stretching of the Na−O distances.

The monoclinic structure of $Na_2U_2O_7$, in space group $P2_1$, was supported by our X-ray diffraction studies and a ^{23}Na MQMAS experiment, which confirmed the existence of two Na sites with chemical shifts at −14.1 (NaO_8) and −19 ppm (NaO_7), respectively. The latter chemical shifts are in the expected range for hexavalent uranium. The thermal expansion coefficients of $Na_2U_2O_7$ were found at $\alpha_a = 6.9 \times 10^{-6}$ K^{-1}, $\alpha_b = 17.3 \times 10^{-6}$ K^{-1}, $\alpha_c = 29.8 \times 10^{-6}$ K^{-1}, and $\alpha_\beta = -9.5 \times 10^{-6}$ K^{-1} in the temperature range 298−573 K.

Finally, first-principles calculations were performed on the compounds Na_4UO_5 and $Na_2U_2O_7$, which have no unpaired 5f electrons. A rather simple procedure was used to extract the NMR parameters: the resulting parameters have to be considered as mean values of the distributions that characterize each site. Our predictions, which are in good agreement with the experimental results, are very encouraging and clearly validate the use of DFT-NMR calculations for f^0 systems and for future investigations.

EXPERIMENTAL SECTION

Raw Materials and Solid-State Synthesis. The $NaUO_3$ and Na_4UO_5 compounds were kindly provided by NRG (Nuclear Research and Consultancy Group, Petten, The Netherlands). $Na_2U_2O_7$ was synthesized by a reaction between depleted uranium oxide (UO_2 from JRC-ITU stocks) and sodium carbonate (Na_2CO_3 99.95%, Sigma) at 1123 K under an oxygen flow in a tubular furnace followed by an annealing treatment at 500 K for 48 h. The starting uranium oxide, being hyperstoichiometric,[34,35] was first reduced to stoichiometry under an Ar/6% H$_2$ flow at 993 K for 8 h. The X-ray patterns recorded revealed a cubic fluorite structure with the cell parameter 5.468(7) Å, in very good agreement with the value reported in the literature of 5.468(7) Å,[35] indicating that the uranium oxide was pure and stoichiometric after thermal treatment.

Room-Temperature X-ray Diffraction. The crystal structures of the compounds were determined at room temperature by X-ray diffraction (XRD) using a Bruker D8 X-ray diffractometer mounted in a Bragg−Brentano configuration with a curved Ge monochromator (111) and a ceramic copper tube (40 kV, 40 mA) equipped with a LinxEye position sensitive detector. The data was collected by step scanning in the angle range $10° \leq 2\theta \leq 120°$, with an integration time of about 8 h, a count step of 0.02 (2θ), and a dwell of 5 s/step. The sample preparation for XRD analysis consisted of dispersing the powder on the surface of a silicon wafer with 2 or 3 drops of isopropyl alcohol. Structural analysis was performed by the Rietveld method with the Fullprof2k suite.[36]

High-Temperature X-ray Diffraction. The thermal stabilities of all three compounds were also assessed by high-temperature X-ray diffraction using a Bruker D8 X-ray diffractometer mounted with a curved Ge monochromator (111), a copper ceramic X-ray tube (40 kV, 40 mA), and a Vantec position-sensitive detector and equipped with an Anton Paar HTK 2000 chamber. Measurements were conducted in helium up to 1273 K. From these data, some reactions of decomposition were characterized and the material's coefficients of thermal expansion calculated.

X-ray Absorption Near-Edge Structure (XANES). XANES measurements were performed at the Rossendorf BeamLine (ROBL) of the European Synchrotron Radiation Facility (ESRF, Grenoble, France).[37] Small amounts (5−10 mg) of powdered sample were mixed with boron nitride (BN) and pressed into pellets for the transition measurements. The storage ring operating conditions were 6.0 GeV and 170−200 mA. A double crystal monochromator mounted with an Si(111) crystal coupled to collimating and focusing Rh coated mirrors was used. XANES spectra were collected at room temperature in transmission mode at the U-L$_{III}$ edge. A step of 0.5 eV was used in the edge region. The E_0 values were taken at the first inflection point by using the first node of the second derivative. The position of the white-line maximum was selected from the first node of the first derivative. Several acquisitions were performed on the same sample and summed to improve the signal to noise ratio. Before averaging scans, each spectrum was aligned using the XANES spectra of the metallic Y foil (17038 eV). The ATHENA software[38] was used to remove the background and normalize the spectra.

^{23}Na Magic Angle Spinning (MAS) Nuclear Magnetic Resonance (NMR). *Experimental Methods.* The ^{23}Na MAS NMR spectra were measured at a Larmor frequency of 105.8 MHz on the 9.4 T spectrometer installed at the JRC-ITU (Joint Research Centre-Institute for Transuranium Elements). This one of a kind spectrometer allows measurement of high-resolution MAS NMR spectra of actinide-bearing compounds.[39] A 4 mm probe was used for the $NaUO_3$ and Na_4UO_5 compounds, and the rotor was spun at 15 kHz. For $Na_2U_2O_7$, the NMR measurements were conducted with a 1.3 mm probe at a MAS rate of 55 kHz. A radio frequency field of 42 kHz ($\pi/2$, 48 transients with a 0.5 s relaxation delay) was applied to be in the selective excitation regime. The ^{23}Na RIACT MQMAS experiments[40,41] carried out on $Na_2U_2O_7$ were acquired with optimized excitation and reconversion pulses $p_1 = 2.5$ μs and $p_2 = 4.5$ μs. Chemical shifts were referenced to 1 M NaCl(aq). Spectra were fitted using the dmfit software.[42]

Theoretical Methods. First-principles calculation of the NMR parameters and geometry optimizations (atomic positions and cell parameters) of the nonmagnetic crystalline compounds Na_4UO_5 and $Na_2U_2O_7$ were performed using the QUANTUM ESPRESSO package,[43] which relies on a pseudopotential plane-wave expansion formalism of density functional theory (DFT). [23]Na electric field gradient (EFG) and magnetic shielding tensors were computed using the projector augmented wave (PAW)[44] and the gauge including projector augmented wave approach (GIPAW)[10,45] formalisms, respectively, using the generalized gradient approximation (GGA) PBE functional.[46] Core electrons were described by norm-conserving Trouiller−Martins pseudopotentials[47] and generated with the atomic code (http://www.quantum-espresso.org) using the parameters given in Table 4. Before the NMR parameters were computed, their

Table 4. Parameters Involved in the Pseudopotential Generation

nucleus	configuration	cutoff radii (au)
Na	$2s^2 2p^6$	1.80, 1.49, 1.80
O	$2s^2 2p^3$	1.45, 1.45
U	$6s^2 6p^6 6d^1 5f^3 7s^0$	1.26, 1.52, 2.20, 1.26

structures were optimized. For all calculations a $3 \times 3 \times 3$ Monkhorst−Pack k-point grid and kinetic cutoff energy of 120 Ry were used (NMR parameters are converged by <0.5 ppm and <0.05 MHz). As the optimized unit cell volumes were overestimated[48] by about 4%, the optimized lattice parameters were rescaled (isotropic rescaling) so as to span a unit cell with the experimental volume.

The isotropic chemical shift, δ_{iso}, was obtained from the isotropic magnetic shielding, σ_{iso} (with $\sigma_{iso} = 1/3 Tr\{\vec{\sigma}\}$), using the following equation: $\delta_{iso} = -(\sigma_{iso} - \sigma_{ref})$.

As the [23]Na is a quadrupolar nucleus (i.e., nuclear spin $I = 3/2$, greater than 1/2 possess a nonvanishing nuclear quadrupolar moment, denoted Q) it is subjected to the quadrupolar interaction. The latter is characterized by two constants: its (quadrupolar) coupling constant C_Q and its asymmetry parameter η_Q (which measures the deviation of the EFG from a cylindrical symmetry $\eta_Q = 0$ ($1 \geq \eta_Q \geq 0$). These parameters are linked with the electric field gradient tensor through $C_Q = (eQV_{zz}/h)$ and $\eta_Q = V_{xx} - V_{yy}/V_{zz}$. The V_{ii} values are the eigenvalues of the (traceless symmetric) EFG tensor ordered according to $|V_{zz}| \geq |V_{yy}| \geq |V_{xx}|$ and Q is the nuclear quadrupole moment $Q(^{23}Na) = 0.104 \times 10^{-28}$ m^2.[49]

Differential Scanning Calorimetry. Differential scanning calorimetry measurements were performed with a SETARAM MDHTC96 apparatus equipped with a furnace and a detector monitoring the difference in heat flow between sample and reference crucibles. The $Na_2U_2O_7$ material (55.0 mg) was encapsulated for the measurement in a stainless steel crucible with a screwed bolt to avoid vaporization, as described in another publicaion.[50] The crucible was brought up to 923 K with heating rates (and respective cooling rates) of 5, 7, and 10 K/min successively. The temperature was monitored throughout the experiment by a series of interconnected S-type thermocouples.

ASSOCIATED CONTENT

Ⓢ Supporting Information

Text, tables, figures, and CIF files giving X-ray crystallographic data, a detailed description of the room-temperature X-ray diffraction characterization of $NaUO_3$, Na_4UO_5, and $Na_2U_2O_7$, ^{23}Na MAS NMR and MQMAS spectra of $NaUO_3$, and thermal expansion data of $NaUO_3$, Na_4UO_5, and $Na_2U_2O_7$. This material is available free of charge via the Internet at http://pubs.acs.org.

AUTHOR INFORMATION

Corresponding Author

*E-mail: anna.smith@ec.europa.eu (A.L.S.); philippe.raison@ec.europa.eu (P.E.R.).

Notes

The authors declare no competing financial interest.

REFERENCES

(1) 2009 GIF R&D Outloook for Generation IV Nuclear Energy Systems, 2009.

(2) Housseau, M.; Dean, G.; Perret, F. *Behaviour and Chemical State of Irradiated Ceramic Fuels, Panel Proceedings Series*; IAEA: Vienna, 1974; p 349.

(3) Blackburn, P.; Hubbard, W. *Proceedings of Conference on Fast Reactor Fuel Element Technology*; Vol. III, American Nuclear Society: Hinsdale, IL, 1972; p 479.

(4) Housseau, M.; Dean, G.; Marcon, J.-P.; Marin, J. *Report CEA-N-1588 (Commissariat à l'énergie atomique et aux énergies alternatives)*; France, 1973.

(5) Smith, A. L.; Raison, P. E.; Suard, E.; Martel, L.; Charpentier, T.; Somers, J.; Wallez, G.; Benes, O.; Apostolidis, C.; Cheetham, A. K.; Konings, R. J. M. *in preparation*.

(6) Smith, A. L.; Raison, P. E.; Konings, R. J. M. *J. Nucl. Mater.* **2011**, *413*, 114−121.

(7) Bykov, D.; Raison, P.; Apostolidis, C.; Konings, R. J. M. *Submitted to J. Nucl. Mater.*.

(8) Pankajavalli, R.; Chandramouli, V.; Anthonysamy, S.; Ananthasivan, K.; Ganesan, V. *J. Nucl. Mater.* **2012**, *420*, 437−444.

(9) Xue, X.; Stebbins, J. F. *Phys. Chem. Miner.* **1993**, *20*, 297−307.

(10) Pickard, C. J.; Mauri, F. *Phys. Rev. B* **2001**, *63*, 245101.

(11) Cho, H.; de Jong, W. A.; Soderquist, C. Z. *J. Chem. Phys.* **2010**, *132*, 084501.

(12) Van den Berghe, S.; Leenaers, A.; Ritter, C. *J. Solid State Chem.* **2004**, *177*, 2231−2236.

(13) Roof, I. P.; Smith, M. D.; zur Loye, H.-C. *J. Cryst. Growth* **2010**, *312*, 1240−1243.

(14) Saine, M.-C. *J. Less-Common Met.* **1989**, *154*, 361−365.

(15) Gasperin, M. *J. Less-Common Met.* **1986**, *119*, 83−90.

(16) Shannon, R. D. *Acta Crystallogr., Sect. A* **1976**, *32*, 751−767.

(17) Conradson, S. D.; Manara, D.; Wastin, F.; Clark, D. L.; Lander, G. H.; Morales, L. A.; Rebizant, J.; Rondinella, V. V. *Inorg. Chem.* **2004**, *43*, 6922−6935.

(18) Soldatov, A. V.; Lamoen, D.; Konstantinovic, M. J.; Van den Berghe, S.; Scheinost, A. C.; Verwerft, M. *J. Solid State Chem.* **2007**, *180*, 54−61.

(19) George, A.; Sen, S.; Stebbins, J. *Sol. State. Nucl. Mag.* **1997**, *10*, 9−17.

(20) Mackenzie, K. J. D.; Smith, M. E. In *Multinuclear Solid-State NMR of Inorganic Materials*; Cahn, R., Ed.; Elsevier: Amsterdam, 2002; Pergamon Materials Science Vol. 6, pp 3−727.

(21) Veron, E.; Garaga, M. N.; Pelloquin, D.; Cadars, S.; Suchomel, M.; Suard, E.; Massiot, D.; Montouillout, V.; Matzen, G.; Allix, M. *Inorg. Chem.* **2013**, *52*, 4250−4258.

(22) Wallez, G.; Raison, P. E.; Dacheux, N.; Clavier, N.; Bykov, D.; Delevoye, L.; Popa, K.; Bregiroux, D.; Fitch, A.; Konings, R. J. M. *Inorg. Chem.* **2012**, *51*, 4314−4322.

(23) Ashbrook, S. E.; Le Pollès, L.; Gautier, R.; Pickard, C. J.; Walton, R. I. *Phys. Chem. Chem. Phys.* **2006**, *8*, 3423−3431.

(24) Bickel, M.; Kanellakopulos, B. *J. Solid State Chem.* **1993**, *107*, 273−284.

(25) Cheetham, A. K.; Dobson, C. M.; Grey, C. P.; Jakeman, R. J. B. *Nature* **1987**, *328*, 706−707.

(26) Aldi, K. A.; Cabana, J.; Sideris, P. J.; Grey, C. P. *Am. Mineral.* **2012**, *97*, 883.

(27) Vosegaard, T.; Florian, P.; Grandinetti, P. J.; Massiot, D. *J. Magn. Reson.* **2000**, *143*, 217−222.

(28) Fenzke, D.; Freude, D.; Fröhlich, T.; Haase, J. *Chem. Phys. Lett.* **1984**, *111*, 171−175.

(29) Angeli, F.; Charpentier, T.; Faucon, P.; Petit, J.-C. *J. Phys. Chem. B* **1999**, *103*, 10356−10364.

(30) Bonhomme, C.; Gervais, C.; Babonneau, F.; Coelho, C.; Pourpoint, F.; Azas, T.; Ashbrook, S. E.; Griffin, J. M.; Yates, J. R.; Mauri, F.; Pickard, C. J. *Chem. Rev.* **2012**, *112*, 5733−5779.

(31) Sali, S. K.; Kulkarni, N. K.; Singh Mudher, K. D. *J. Alloys Compd.* **2006**, *425*, 28−33.

(32) Cordfunke, E. H. P.; Muis, R. P.; Ouweltjes, W.; Flotow, H. E.; O'Hare, P. A. G. *J. Chem. Thermodyn.* **1982**, *14*, 313−322.

(33) Momin, A. C.; Mirza, E. B.; Mathews, M. D. *J. Nucl. Mater.* **1991**, *185*, 308−310.

(34) Guéneau, C.; Chartier, A.; Brutzel, L. V. *Comprehensive Nuclear Materials*; Elsevier: Amsterdam, 2012; Vol. 2, Chapter 2.

(35) Desgranges, L.; Baldinozzi, G.; Rousseau, G.; Nièpce, J.-C.; Calvarin, G. *Inorg. Chem.* **2009**, *48*, 7585−7592.

(36) Rodriguez-Carvajal, J. *Physica B* **1993**, *192*, 55−69.

(37) Matz, W.; Schell, N.; Bernhard, G.; Prokert, F.; Reich, T.; Claussner, J.; Oehme, W.; Schlenk, R.; Dienel, S.; Funke, H.; Eichhorn, F.; Betzl, M.; Pröhl, D.; Strauch, U.; Hüttig, G.; et al. *J. Synchrotron Radiat.* **1999**, *6*, 1076−1085.

(38) Ravel, B.; Newville, M. *J. Synchrotron Radiat.* **2005**, *12*, 537−541.

(39) Martel, L.; Somers, J.; Berkmann, C.; Koepp, F.; Rothermel, A.; Pauvert, O.; Selfslag, C.; Farnan, I. *Rev. Sci. Instrum.* **2013**, *84*, 055112.

(40) Wu, G.; Rovnyak, D.; Griffin, R. G. *J. Am. Chem. Soc.* **1996**, *118*, 9326−9332.

(41) Angeli, F.; Charpentier, T.; de Ligny, D.; Cailleteau, C. *J. Am. Ceram. Soc.* **2010**, *93*, 2693−2704.

(42) Massiot, D.; Fayon, F.; Capron, M.; King, I.; Calvé, S. L.; Alonso, B.; Durand, J.-O.; Bujoli, B.; Gan, Z.; Hoatson, G. *Magn. Reson. Chem.* **2002**, *40*, 70−76.

(43) Giannozzi, P.; Baroni, S.; Bonini, N.; Calandra, M.; Car, R.; Cavazzoni, C.; Ceresoli, D.; Chiarotti, G. L.; Cococcioni, M.; Dabo, I.; Dal Corso, A.; de Gironcoli, S.; Fabris, S.; Fratesi, G.; Gebauer, R.; et al. *J. Phys.: Condens. Matter* **2009**, *21*, 395502.

(44) Bloechl, P. *Phys. Rev. B* **1994**, *50*, 17953.

(45) Charpentier, T. *Solid State NMR* **2011**, *40*, 1−20.

(46) Perdew, J. P.; Burke, K.; Ernzerhof, M. *Phys. Rev. Lett.* **1996**, *77*, 3865−3868.

(47) Trouiller, N.; Martins, J. *Phys. Rev. B* **1991**, *43*, 1993.

(48) Charpentier, T.; Ispas, S.; Profeta, M.; Mauri, F.; Pickard, C. J. *J. Phys. Chem. B* **2004**, *108*, 4147−4161.

(49) Pyykko, P. *Mol. Phys.* **2008**, *106*, 1965−1974.

(50) Benes, O.; Konings, R. J. M.; Wurzer, S.; Sierig, M.; Dockendorf, A. *Thermochim. Acta* **2010**, *509*, 62−66.